

Shape of the Plasma Boundary in TBR

M.E. CONDE, R.M.O. GALVÃO[†], I.C. NASCIMENTO, E.K. SANADA and A.G. TUSZEL
Instituto de Física, Universidade de São Paulo, Caixa Postal 20516, São Paulo, 01498, SP, Brasil

Recebido em 25 de agosto de 1986

Abstract A diagnostic system to determine the shape of the cross-section of the plasma column in TBR-1 has been developed. The system relies on measurements of radial and azimuthal components of the magnetic field around the plasma column and is based upon a technique developed by Swain and Neilson. It is shown that during normal discharges the plasma column undergoes a systematic downward shift and shrinks in minor and major radii.

1. INTRODUCTION

The basic equilibrium characteristics of tokamak discharges are determined through measurements of the toroidal plasma current, toroidal and vertical components of the external magnetic field, and loop voltage. However, more detailed information is needed to study the magnetohydrodynamic stability conditions of the discharges. In this case, it is necessary to determine the shape of the cross section of the plasma column and the radial profiles of the pressure and current density¹. Usually, the pressure profile is inferred from measurements of the electron temperature profile through Thompson scattering and of plasma density through microwave or laser interferometry². The current profile can at present be only indirectly determined.

Many different methods have been developed in the last decade to determine the shape of the cross section of the plasma column²⁻⁹. Although all the methods rely on measurements of the magnetic flux and/or components of the poloidal magnetic field outside the plasma column, they substantially vary in the degree of sophistication to model the current distribution in the plasma. The more accurate methods solve the free-boundary magnetohydrodynamic equilibrium problem¹⁰ and adjust the shape

[†] Also at Instituto de Pesquisas Espaciais, Caixa Postal 515, São José dos Campos, 12200, SP, Brasil.

of the cross section and other free parameters to reproduce external measurements and the pressure profile^{4,5,7,8,9}. Because these methods self-consistently solve the equilibrium problem, they allow not only the determination of the shape of the plasma cross section, but also an indirect determination of the poloidal beta

$$\beta_p = \frac{\frac{1}{V} \int p \, dV}{\frac{1}{2\mu_0} \langle B_p^2 \rangle} \quad (1)$$

the profile of the safety factor,

$$q = B_{T0} R_0 \int_{\psi} \frac{ds}{R^2 B_p} \quad (2)$$

and the internal inductance of the plasma column,

$$L_i = \frac{\frac{1}{V} \int B_p^2 \, dV}{\langle B_p^2 \rangle}$$

In these expressions R is the radial coordinate of a point on a flux surface, R_0 is the major radius of the geometric center of the plasma column, B_p is the poloidal component of the magnetic field, B_{T0} is the toroidal magnetic field at $R = R_0$, p is the plasma pressure, V is the plasma volume, ds is the element of arc length along the poloidal direction of a $\psi = \text{const}$ flux surface, and $\langle \rangle$ represents the average over the plasma cross section¹¹.

The major drawback of methods based upon a self-consistent solution of the magnetohydrodynamic equilibrium equation is that they take a substantial amount of computer time. Although the knowledge of β_p and of the q profile is essential for a stability analysis, an experimentalist usually needs quick information about the value of β_p and the shape of the cross section to properly adjust external parameters between discharges. For this reason, less accurate, swifter, methods have also been developed^{3,6}. These methods are based upon modelling the toroidal plasma current by a set of discrete filaments whose positions are a priori fixed. The currents in these filaments are calculated from the minimization of the average square deviation of measured and calculated values of the magnetic field at the positions of diagnostic

probes. In particular, Swain and Neilson⁶ have developed a technique that allows a very fast determination of the shape of the cross section of the plasma column and an accurate estimate for the Shafranov parameter¹¹

$$\Lambda = \beta_p + \frac{l_i}{2} \quad (4)$$

In this paper we report the results of measuring the shape of the cross section of the plasma column in the TBR-1 tokamak¹². Previous measurements of resistive modes in TBR-1 have shown a systematic downward displacement of the mode structure^{13,14}. It was not clear whether this displacement occurred only in the perturbation or was caused by a displacement of the equilibrium position of the plasma column as a whole. The measurements carried out with the experimental apparatus described in this paper have found that the plasma column not only shifts downwards during the discharges but also shrinks and increases the internal inductance.

In the next section we present a summary of the technique developed by Swain and Neilson. In section 3 we describe the diagnostic system that has been developed at the Instituto de Física of Universidade de São Paulo. In section 4 we present the main results and the conclusion.

2. ANALYTICAL MODEL

The equilibrium of the plasma column in a tokamak is maintained by the poloidal field created by currents that circulate in the plasma and in external coils¹⁵. The latter produce a magnetic field that in the plasma region is mainly parallel to the symmetry axis of the torus and thus are called vertical field coils. The plasma current, on the other hand, is induced inside the vacuum chamber by the time variation of a magnetic flux through the central hole of the torus. The coils that produce this flux are part of the so-called ohmic heating transformer (OHT)¹⁶. In fig. 1 we show a toroidal cross section of the TBR-1 tokamak showing the vertical field coils, the OHT coils, the vacuum chamber, and the edge of the current limiter. The limiter is a metal ring that limits the current channel and keeps the hot plasma away from the vacuum chamber.

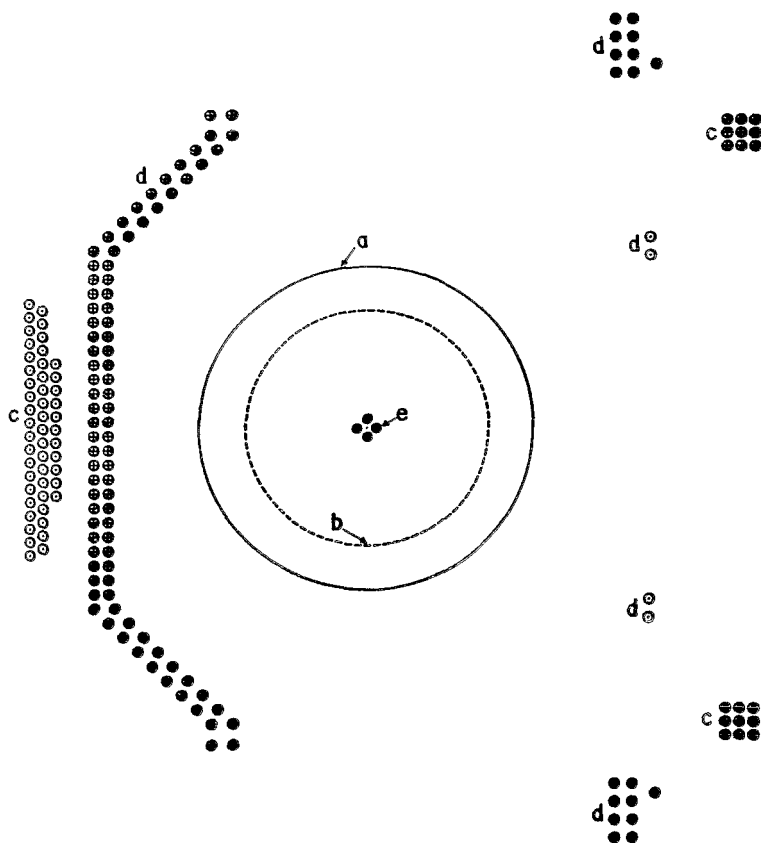


Fig. 1 - Cross section of the TBR-1 tokamak showing the vacuum chamber (a), the edge of the current limiter (b), the vertical field coils (c), the ohmic heating coils (d), and the filaments to simulate the plasma current (e).

Let us assume that outside the current channel, in the shadow of the limiter, we put a set of N pick-up coils that measure in different points the radial and azimuthal components of the magnetic field during a discharge. This field is produced by the plasma current and by the currents in all external coils, which are known. Although the total plasma current can be measured, the profile of the corresponding current density and the shape of the current channel are unknown. The technique of Swain and Neilson⁶ consists in first simulating the plasma current

density by a set of M toroidal filaments located at pre-chosen positions. We shall refer to those filaments as *plasma* filaments; four of them are indicated in fig. 1. Let us denote the current in the external coils by I_j^e and the currents in the *plasma* filaments by I_j^p . The index j runs from 1 to the total number J of external coils in the first case and from 1 to M in the second case. The unknown currents I_j^p are then determined by minimizing the average square deviation of the magnetic field

$$\langle \Delta B^2 \rangle = \frac{1}{N} \sum_{i=1}^N \frac{(B_{ie} - B_{im})^2}{\sigma_i^2}, \quad (5)$$

where B_{ie} and B_{im} are respectively the calculated and measured values of the poloidal (radial and azimuthal components) magnetic field and σ_i is the estimated standard deviation reflecting the measurement uncertainty at sensor i . It can be shown that the minimization of $\langle \Delta B^2 \rangle$ leads to a system of M linear algebraic equations for the unknown currents I_j^p ^{6, 17}

$$\sum_{i=1}^N \frac{B_{im} - B_{ie}}{\sigma_i^2} Q_{ik}^p = \sum_{j=1}^J I_j^p \sum_{i=1}^N \frac{Q_{ij}^p Q_{ik}^p}{\sigma_i^2}, \quad k = 1, 2, \dots, M, \quad (6)$$

where B_{ie} is the total field at position i produced by the currents in the external filaments,

$$B_{ie} = \sum_{j=1}^J Q_{ij}^e I_j^e, \quad (7)$$

and $Q_{\alpha\beta}^{e,p}$ are matrices corresponding to Green's functions, i.e., they give the magnetic field produced at position α by a unit current located at position β . In the present case, all the external coils and *plasma* filaments are concentric circular loops and the expressions for $Q_{\alpha\beta}^{e,p}$ can be readily obtained¹⁸. Since the total plasma current I_p is known, the minimization of $\langle \Delta B^2 \rangle$ can be carried out imposing the constant

$$\sum_{j=1}^M I_j^p = I_p.$$

However, this constraint practically does not change the results obtained without imposing it¹⁷. Actually this occurs because the currents

$I_j^{\mathcal{P}}$ in the *plasma* filaments have no physical meaning. They only approximately give the magnetic field produced by the real plasma current outside the current channel and their first moments correspond to the first moments of the current profile in the plasma⁶.

Once the currents $I_j^{\mathcal{P}}$ are calculated, one can find the flux function $\psi(R,Z) = 2\pi R A_\phi$, where (R,ϕ,Z) are cylindrical coordinates centred at the symmetry axis of the torus and A_ϕ is the toroidal component of the vector potential⁹. Since the plasma boundary has to be a flux surface, to determine the cross section of the plasma column one has to find the flux surface that touches the limiter in just one point. This is carried out by a numerical code that directly plots the plasma cross section¹⁷.

Two important equilibrium quantities can be calculated from the knowledge of the currents $I_j^{\mathcal{P}}$ in the plasma filaments and the shape of the cross section of the plasma column. The first quantity is the radial displacement of the magnetic axis with respect to the geometric center of the plasma cross section, the so-called Shafranov shift¹⁵. This is given by

$$\Delta = \frac{1}{\mu_0 I_p} \oint_c (-\xi B_t + Z B_n) dl \quad (8)$$

where $\xi = R - R_0$ and B_t and B_n are respectively the tangential and normal components of the magnetic field along a closed poloidal contour c around the plasma column². In our case, we choose the contour c to coincide with the edge of the current limiter because along this contour the magnetic field produced by the currents in the *plasma* filaments very closely reproduces the field due to the real current distribution⁶. Equation (8) is derived using a multipole expansion of the plasma current distribution which assumes up-down symmetry with respect to the equatorial plane of the plasma column². In the case of TBR-1, the plasma column is displaced downwards and asymmetric with respect to the equatorial plane. This introduces an additional term into the right-hand side of the above expression for Δ . Assuming that the downward displacement of the plasma column Z_0 is much smaller than the major radius, the correction term is to lowest order given by

$$\frac{Z_0}{\mu_n I} \oint_C B_n d\ell$$

We have calculated this term for TBR-1 discharges and verified that it introduces a correction smaller than 5% in the final value of A ; this correction is of the order of the accuracy of the measurements and thus it has not been taken into account.

The other important equilibrium quantity is the Shafranov parameter A defined in eq. (4). This is calculated using the formula

$$A = \frac{s_1}{2} + s_2 \tag{9}$$

where s_1 and s_2 are two integrals over the plasma surface defined by

$$s_1 = \frac{1}{\mu_0^2 R I_p^2} \int B_t^2 \rho \hat{n} \cdot \hat{e}_\rho dS_n \tag{10}$$

and

$$s_2 = \frac{1}{\mu_0^2 I_p^2} \int B_t^2 \hat{n} \cdot \hat{e}_R dS_n, \tag{11}$$

where ρ is the radial variable of a pseudo-toroidal coordinate system centred at the magnetic axis of the plasma column and \hat{e}_ρ and \hat{e}_R are unit vectors in the directions $\rho = \text{const.}$ and $R = \text{const.}$, respectively¹¹. The integrals appearing in eqs. (8), (10), and (11) are calculated using a numerical code described in reference 17.

To test the accuracy of the method and to determine the optimal number M of plasma filaments, we have carried out numerical simulations of real plasma discharges assuming a parabolic current density profile and using twenty diagnostic coils, corresponding to the actual diagnostic system. The field produced at the position of each diagnostic coil has been calculated and multiplied by a random factor between 0.9 and 1.1 to simulate experimental errors in real measurements. We have found out that a very good approximation to the exact shape of the plasma cross-section can be obtained using three to six plasma filaments ($3 \leq M \leq 6$). Details of the simulations are given in reference 17.

Finally, we have slightly improved the technique of Swain and Neilson to better accommodate the displacement of the plasma column in TER-1. The positions of the *plasma* filaments are initially chosen with their geometric center coinciding with the one of the vacuum chamber. If the geometric center of the plasma cross section is found to be shifted with respect to the center of the vacuum chamber, the center of the *plasma* filaments are shifted to that position and the whole calculation repeated. This process goes on until the displacement between two subsequent positions of the center of the plasma cross section is smaller than 0.5 mm. In practice we find that no more than two iterations are sufficient to satisfy this criterion.

3. DIAGNOSTIC SYSTEM

The TBR-1 tokamak is a small-size device that has been designed and constructed at the *Instituto de Física* of *Universidade de São Paulo*¹². Reproducible discharges are obtained after approximately five hours of discharge or radio-frequency cleaning^{20,21}. The plasma current can be varied from 6 to 12 kA, with pulse duration up to 7ms, and the toroidal magnetic field can be varied from 4 to 5 kG. The vacuum chamber (316 LSS) is 3 mm thick, which gives an attenuation of approximately 13 db for signals in the kHz range. Therefore, we have designed the diagnostic system with the pick-up coils inside the vacuum chamber to prevent attenuation and distortion of the signals.

Two types of coils are used: the radial coils that measure the radial component of the poloidal magnetic field and the tangential coils that measure the azimuthal component. The tangential coils are made of 56 turns of ϕ 0.13 mm copper wire directly wound on two ϕ 12.7 mm nylon tubes. The radial coils are made of 130 turns of the same wire wound on small spools that are then inserted in transversal orifices in the nylon tubes. The size of the coils and the assembling scheme are indicated in fig. 2a. The two nylon tubes are then covered with heat-shrink isolation, bent in semicircles of 9.7 mm radius (fig. 2b), and inserted into stainless steel semicircular tubes of 19 mm internal diameter and 0.3 mm thickness. One end of these supporting tubes is closed with a vacuum tight metal plug and the other end is soldered to a straight

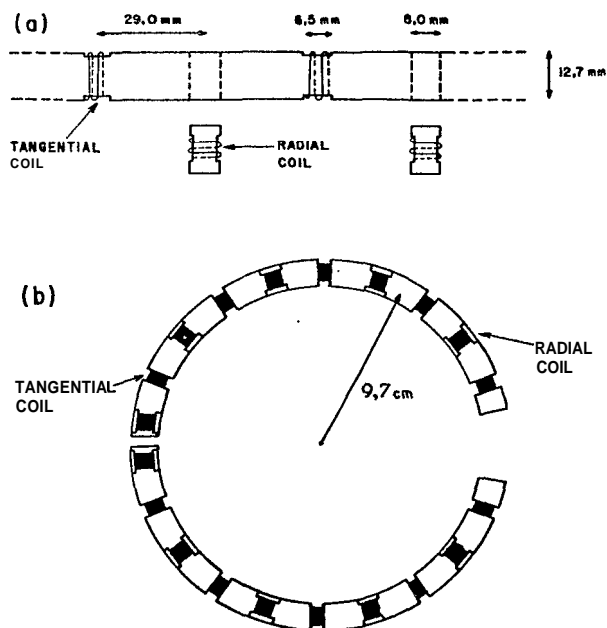


Fig.2 - Sketch of the tangential and radial pick-up coils and the assembling scheme (a) and the two bent nylon tubes before insertion in the supporting metal tubes (b).

tube that can slide inside a feedthrough in the vacuum flange (fig. 3).

During discharge cleaning, the vacuum chamber and metal surfaces inside it get very hot. In order to avoid melting of the isolation of the pick-up coils, cooling air is forced into the nylon tube and returns through the space between the nylon and supporting tubes, as indicated in fig. 3b. A picture of the entire assembly is shown in fig. 4. This type of construction considerably facilitates the insertion of the diagnostic system into the vacuum chamber, in spite of the small size of the diagnostic ports of TBR-I. By rotating the supporting tubes, the two semi-circles can be brought close together and then inserted into the vacuum chamber. Once the flange is in place, the two tubes are rotated back to the proper positions.

The effective areas of the pick-up coils have been determined

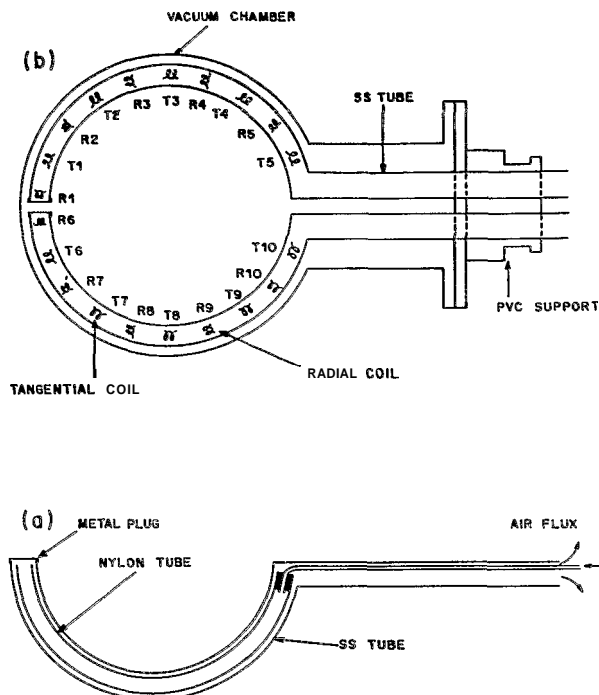


Fig.3 - Sketch of the stainless steel supporting tubes showing the refrigeration system (a) and position of the pick-up coils inside the vacuum chamber (b).

in a standard Helmholtz coil fed with a 60 Hz cw current. The measured values are given in table 1. In the actual experiment, the signal of each coil has to be integrated. We have designed a very versatile active integrator that can operate either as differential or unipolar amplifier¹⁷. There is one integrator for each coil. The signals from the integrators are digitalized in *Le Croy* 2264 modules and stored in *Le Croy* 8800A and 8800/8 memories for later displaying in an oscilloscope or further computer processing. The reading rate of the modules is fixed at 2.5 μ s. The gains of the integrators have been calibrated using a known input signal and a 50R load, corresponding to the input impedance of the CAMAC modules. The actual gains used for each coil are shown in table 1.

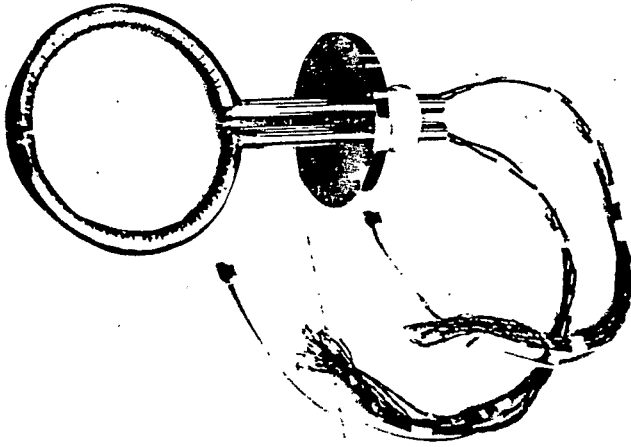


Fig. 4 - Picture of the diagnostic system.

The toroidal magnetic field in TBR-1 has a strong ripple due to the discreteness of the toroidal field coils²². This produces a radial magnetic field component that is detected by the radial pick-up coils. The corresponding signal is so intense that it completely saturates the CAMAC modules. To eliminate this effect, we have added a constant dc voltage to the output of the active integrators that are connected to the radial diagnostic coils. Furthermore, we correct the signal of these coils by subtracting out the spurious signal that is measured in the absence of plasma, by pulsing only the toroidal field coils.

4. RESULTS

We have analysed various discharges in TBR-1 with the plasma current varying from 5.5 to 10.5 kA and with a discharge duration of approximately 6.5 ms. In this paper we report the results obtained for two discharges, one with a current of 8.7 kA and the other with a current of 10 kA. These discharges are typical within the range of parameters that have been used. Discharges with currents smaller than 9 kA usually have a low magnetohydrodynamic activity whereas discharges with currents above 10 kA have strong activity¹⁴.

Table 1 - Effective area of the pick-up coils and gain of the integrators used in each coil. The labels of the coils correspond to the labels used in fig. 3a.

radial coil	effective area (10^{-3} m^2) (± 0.08)	gain (s^{-1}) $G = \frac{V_{out}}{\int V_{in} dt}$	tangential coil	effective area (10^{-3} m^2) (± 0.08)	gain (s^{-1}) $G = \frac{V_{out}}{\int V_{in} dt}$
R1	5.31	3.98	T1	5.55	817
R2	5.59	4.06	T2	5.97	707
R3	5.69	4.14	T3	5.96	818
R4	5.34	4.51	T4	5.74	846
R5	5.59	4.18	T5	5.96	964
R6	5.48	3.64	T6	6.06	885
R7	5.14	6.00	T7	5.62	771
R8	5.42	3.92	T8	5.64	871
R9	5.42	4.19	T9	6.04	850
R10	5.47	3.99	T10	6.05	919

To illustrate the experimental procedure, we will give the raw data only for the 8.7 kA discharge; the data for the other discharge are quite similar. In fig. 5 we show the main parameters of the discharge; namely, loop voltage, plasma current, radial position of the plasma column, hard X-ray emission, and currents in the vertical field and ohmic heating coils. The radial position of the plasma column is globally measured by sensing coils outside the vacuum chamber^{2,3}. The signals detected by the pick-up coils are shown in fig. 6 for the azimuthal and in fig. 7 for the radial coils. We note that whereas the signals of the azimuthal coils very closely resemble the signal of the total plasma current, as they should, the signals of the radial coils seem very distorted, due to the ripple of the toroidal magnetic field, as previously mentioned. This can be seen by the signals detected by the radial coils when only the toroidal coils are pulsed, without plasma. These signals are also shown in fig. 7.

Using the values of the poloidal magnetic field measured by the

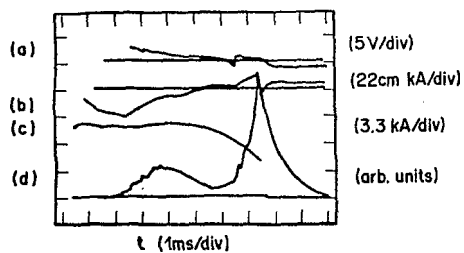


Fig.5 - Main parameters of the 8.7 kA discharge: loop voltage (a), radial position (b), plasma current (c), hard X-ray emission (d), current in ohmic heating transform (e), and current in the vertical field coils (f).

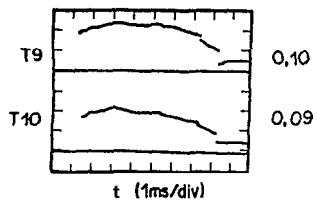
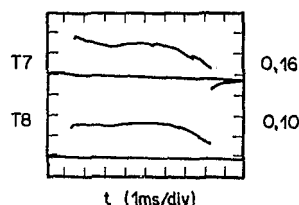
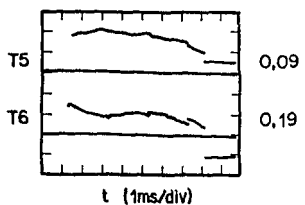
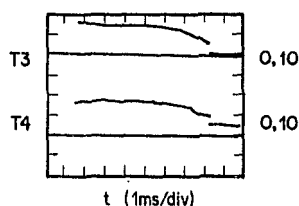
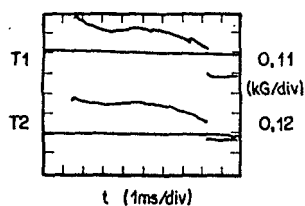
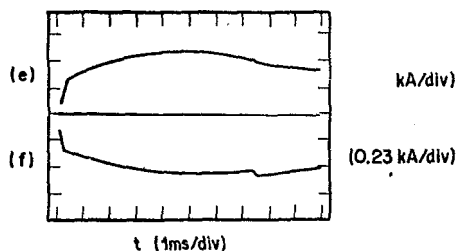


Fig.6 - Field measured by the tangential field coils in the 8.7 kA discharge. The labels T1 to T10 correspond to the coils whose positions are indicated in fig. 3b.

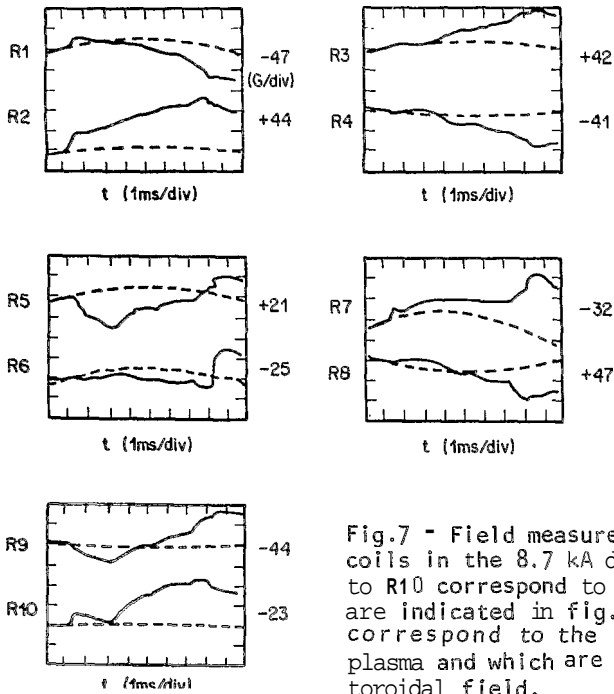


Fig.7 - Field measured by the radial field coils in the 8.7 kA discharge. The labels R1 to R10 correspond to the coils whose positions are indicated in fig. 3b. The dashed lines correspond to the signals obtained without plasma and which are due to the ripple of the toroidal field.

pick-up coils, we can determine the plasma cross section and other equilibrium quantities, as discussed in section 2. The time evolution of the shape of the plasma cross section is shown in figs. 8 and 9 for 8.7 and 10 kA discharges, respectively. In the former case, the plasma column is first displaced towards the outside of the torus and then towards the inside. For the latter, the plasma column is continuously displaced towards the inside of the torus. In both cases, however, the plasma column shows a downward displacement and shrinks in minor radius towards the end of the discharge. The radial displacement of the plasma column can be more quantitatively seen by plotting the position of the geometric center of the plasma filaments as a function of time. This is shown in fig. 10. In the same picture we also show the position of the plasma column as measured by the radial position coils^{2,3}. It is clear that although the two measurements qualitatively agree, there is a constant shift between the two results. This is probably due to a small asymmetry in the radial position coil. If we correct for this asymmetry by making

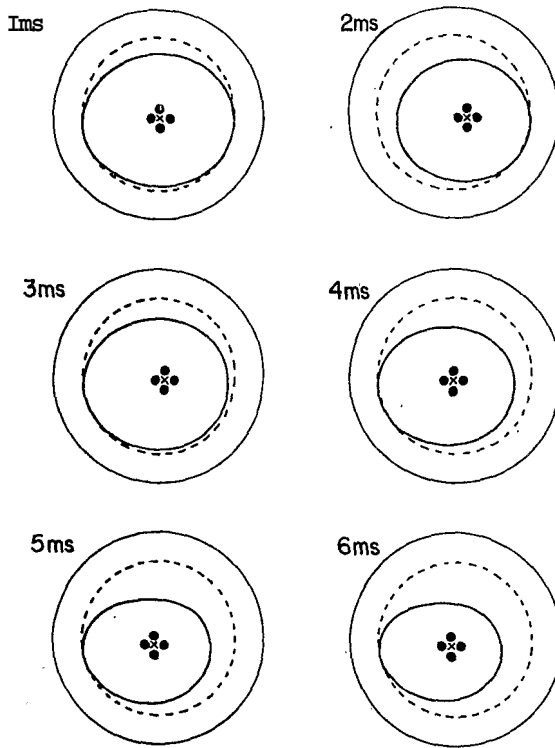


Fig.8 - Time evolution of the cross section of the plasma column in the 8.7 kA discharge. Four filaments were used to simulate the plasma current. The x denotes the position of the geometric center of the filaments. The symmetry axis of the torus is to the left of the figures. Time is computed from the beginning of the discharge.

a uniform shift in the results of these coils, the two sets of measurements also quantitatively agree¹⁷.

The downward displacement of the plasma column can be seen by plotting the vertical position of the geometric center of its cross section as a function of time. This is shown in fig. 11. We see that the plasma column is almost one centimeter downward displaced at the

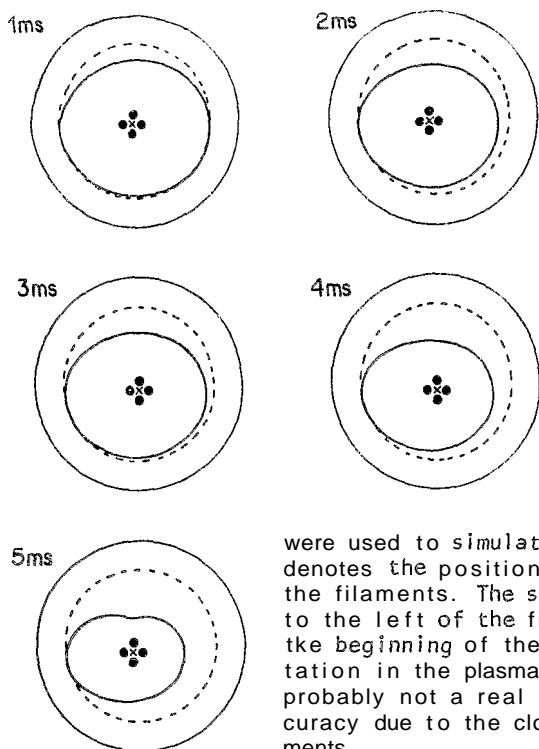


Fig.9 - Time evolution of the cross section of the plasma column in the 10 kA discharge. Four filaments were used to simulate the plasma current. The x denotes the position of the geometric center of the filaments. The symmetry axis of the torus is to the left of the figures. Time is computed from the beginning of the discharge. The small indentation in the plasma cross section at $t = 5 \text{ ms}$ is probably not a real feature but a numerical inaccuracy due to the closeness of the plasma filaments.

end of the discharge. Considering that the initial minor radius of the plasma column is only 8 cm, this displacement is quite substantial. Furthermore, it makes the hot plasma strongly interact with the current limiter, producing the copious hard X-ray emission shown in fig. 5 at the end of the discharge. The compression of the plasma column in both minor and major radii is probably due to the value of the external vertical field becoming larger than necessary. The downward displacement, on the other hand, is probably due to an asymmetry in the vertical field coils or incomplete cancellation of the vertical stray field produced by the toroidal field coils. This downward displacement has also been measured by Ueta using sensing coils outside the vacuum chamber²³.

Because the total plasma current is kept approximately constant and the cross section of the plasma column diminishes during the

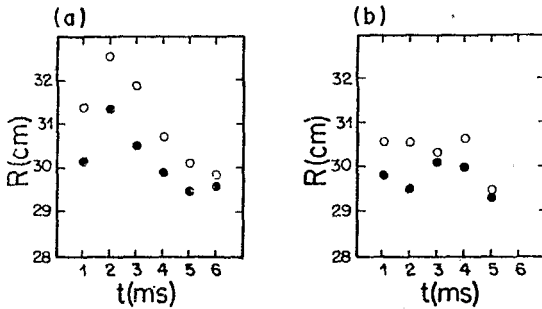


Fig.10 - Radial position of the geometric center of the *plasma* filaments (●) as a function of time for the 8.7 kA (a) and 10 kA (b) discharges. The open circles represent the center of the plasma column determined from the radial position coils^{2,3}.

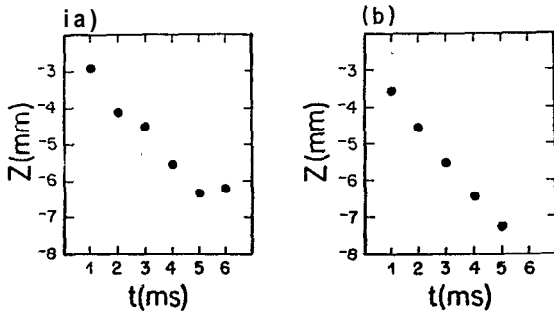


Fig.11 - Vertical position of the geometric center of the plasma cross section as a function of time for the 8.7 kA (a) and 10 kA (b) discharges.

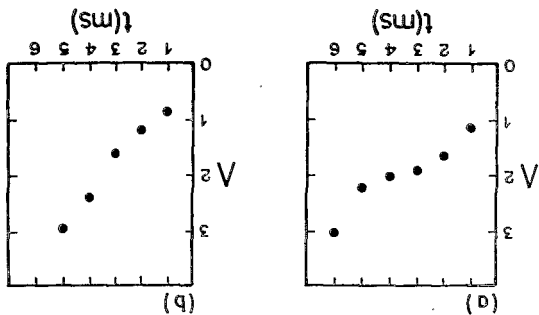
discharge, the current density profile has to become steeper, increasing the internal inductance R_z (eq.(3)). This is seen in fig. 12 where the parameter Λ (eq. (4)) is plotted as a function of time. Clearly, the value of Λ can also increase due to an increase in the value of β_p , caused by compressional heating by the vertical inagnetic field. The maximum possible heating occurs under the condition of adiabatic compression. In this case, conservation of poloidal and toroidal magnetic

We thank Dr. A. Wootton for useful discussions. This work has been supported by *Fundação de Amparo à Pesquisa do Estado de São Paulo* and *Emancipadora de Estudos e Projetos*.

We conclude that the diagnostic system described in this paper can provide an accurate and fast determination of the shape of the cross section of the plasma column and other relevant equilibrium quantities in tokamak discharges. Knowing the shape of the cross section, the total plasma current, and the values of Δ and Λ , one can use a magnetohydrodynamic equilibrium code to solve the fixed boundary equilibrium problem (which is much simpler than the free-boundary one¹⁰) and obtain consistent profiles for the pressure and current density in the plasma.

fluxes imposes the value of B_p^d to scale as $B_p^d \sim a^{-4/3} R^{1/3}$, where a is the average minor radius of the plasma cross section, whereas the value of λ_z remains constant. If a decreases faster than R , the value of B_p^d can increase. However, for our conditions, it can be easily shown that heating by magnetic compression cannot account for the observed large increase in the value of Λ , whereas a mild peaking of the current density profile can substantially increase the value of the internal inductance λ_z^{17} .

Fig. 12 - Time evolution (●) of the equilibrium quantity $\Lambda = B_p + \lambda_z^2/2$ for the 8.7 kA (a) and 10 kA (b) discharges.



REFERENCES

1. N.C.Luhmann Jr. and W.A.Peebles, *Rev.Sci.Instrum.* 55, 279 (1984).
2. L.E.Zakharov and V.D.Shafranov, *Sov.Phys.Tech.Phys.* 18, 151 (1973).
3. A.J.Wootton, *Nuc. Fusion* 19, 987 (1979).
4. G.N.Deshko, T.G.Kilovataya and Yu.K.Kuznetsov, *Nuc. Fusion* 23, 1309 (1983).
5. S.P.Bondarenko, V.E.Golant and M.P.Gryaznevich, *Sov. J. Plasma Phys* 10, 520 (1984).
6. D.W.Swain and G.N.Neilson, *Nucl.Fusion* 22, 1015 (1982).
7. J.L.Luxon and B.B.Brown, *Nucl. Fusion* 22, 813 (1982).
8. L.L.Lao, H.St. John, R.D.Stambough and W.Pfeiffer, *Nucl. Fusion* 25, 1421 (1985).
9. W.Feneberg, K.Lackner and P.Martin, *Comp.Phys.Commun.* 31, 143 (1984).
10. G.Genacchi, R.M.O.Galvão and A.Taroni, *Nucl.Fusion* 16, 457 (1976).
11. V.D.Shafranov, *Plasma Phys.* 13, 757 (1971).
12. I.C.Nascimento, A.N.Fagundes, R.P.da Silva, R.M.O. Galvão, E. del Bosco, J.H.Vuolo, E.K.Sanada and R.Dallaqua, in *Fusion Energy-1981*, Selected Lectures presented at a Spring College on Fusion Energy, International Centre for Theoretical Physics, Trieste 1982, p.45.
13. I.H.Tan, I.L.Caldas, I.C.Nascimento, R.P.Silva, E.K.Sanada and K. Bruha, *Proceedings of the 1984 International Conference on Plasma Physics*, Ecole Polytechnique Fédérale de Lausanne, Lausanne 1984, Vol. I, p. 72.
14. I.H.Tan, I.L.Caldas, I.C.Nascimento, R.P.da Silva, E.K.Sanada and R.Bruha, to be published in *IEEE trans. on Plasma Science* (1986).
15. V.D.Shafranov, *Sov. Phys. Tech. Phys.* 15, 175 (1970).
16. L.A.Artsimovich, *Nucl.Fusion* 12, 215 (1972).
17. M.E.Conde, "Determinação da Seção Transversão da Coluna de Plasma no Tokamak TBR-I", *MSc. Thesis*, Instituto de Física, Universidade de São Paulo, São Paulo, June 1986.
18. W.R.Smithe, *Static and Dynamic Electricity*, McGraw-Hill, New York (1950), Chap. 7.
19. V.D.Shafranov, in *Reviews of Plasma Physics*, Ed. M.A.Leotovich, Consultants Bureau, New York (1966), Vol. 2, p. 103.

20. L.Oren and R.J.Taylor, Nucl. Fusion 15, 1143 (1979).
21. J.Iraburu Elizondo, "Condicionamento do Tokamak TBR-1 por Plasma Gerado por Microondas", MSc. Thesis, Instituto de Física, Universidade de São Paulo, São Paulo (1986).
22. J.L.Ferreira, "Diagnóstico Básicos de Plasma no TBR", MSc. Thesis, Instituto de Física, Universidade de São Paulo, São Paulo (1980).
23. A.Y.Ueta, "Campo Vertical de Equilíbrio no Tokamak TBR", MSc.Thesis, Instituto de Física, Universidade de São Paulo, São Paulo (1985).

Resumo

Um sistema de diagnóstico para determinar a forma da seção transversal da coluna de plasma no tokamak TBR-1 é descrito. O sistema é baseado numa técnica desenvolvida por Swain e Neilson e utiliza medidas das componentes radial e azimutal do campo magnético na entorno da coluna de plasma. Com este sistema foi verificado que durante descargas normais a coluna de plasma apresenta um deslocamento sistemático para baixo do plano equatorial da máquina e encolhe tanto em relação ao raio maior como ao raio menor.